Desalination and Water Treatment
www.deswater.com

doi: 10.5004/dwt.2019.24125

156 (2019) 96–105
July

Adsorption of Congo red from solution using chitosan modified carbon nanotubes

Weili Wang, Yangyang Du, Mingyu Liu, Mengmeng Yang, Runping Han*

College of Chemistry and Molecular Engineering, Zhengzhou University, No 100 of Kexue Road, Zhengzhou, 450001 China, Tel. +86 371 67781757, Fax +86 371 67781556, email: 1063455250@qq.com (W. Wang), zzudyy@qq.com (Y. Du), lmylittlerain@163.com (M. Liu), 1582415059@qq.com (M. Yang), rphan67@zzu.edu.cn (R. Han)

Received 8 November 2018; Accepted 16 March 2019

ABSTRACT

Chitosan (CS) modified multi-walled carbon nanotubes (MWCNTs) were used as adsorbents (CS-MWCNTs) to adsorb Congo red (CR, anionic dye) from solution in batch mode. The structure and morphology of CS-MWCNTs were characterized by TEM, FTIR, Raman and XPS. The results from analysis of FTIR and XPS showed that CS was successfully loaded onto the MWCNTs. Raman analysis showed that the basic structure of MWCNTs after CS modification did not change. Adsorption studies were performed at different pH, coexisted ions concentrations, contact time and CR concentrations in the batch mode. Results showed that the pH of CR solution at 4.0 was best for the adsorption and the adsorption capacity could reach up to 623 mg·g^{-1} at 303K. The adsorption of the CR solution reached equilibrium within 8 h. Adsorption equilibrium data can be predicted by the Freundlich model while the kinetic adsorption data follow a pseudo-second-order model. Thermodynamic results showed that the adsorption process was spontaneous, and endothermic. The CR-loaded adsorbent can be regenerated using a 0.01 mol·L^{-1} NaOH solution, the regeneration rate can still reach 71% after three cycles. CS-MWCNTs may be available in removal of anionic dyes from solution.

Keywords: CS-MWCNTs; Adsorption; Congo red; Regeneration

1. Introduction

Modern industry, especially the textile industry, emits a large amount of dye wastewater every year. If these wastewaters are directly discharged without treatment, they will cause serious pollution to water bodies [1]. Therefore, it is urgent to purify the dye before discharge of dye solution into environment. The traditional methods of dye wastewater's treatment include coagulation, sedimentation, oxidation, membrane technology, biological treatment and adsorption technique [2,3]. The adsorption method is one common method because of its simplicity, high efficiency, easy recovery, and easy recycling [4]. Various adsorbents such as activated carbons in different forms [5], clays [6] and carbon nanotubes [13] were successfully used to remove dyes from aqueous solution. The most widely used adsorbent for the adsorption process in industrial wastewater treatment systems is activated carbon due to its large specific surface area. Owing to the high cost of activated carbon, the use of this adsorbent is limited. Therefore, researches have been continued for inexpensive alternative adsorbents having reasonable adsorption efficiencies [6].

Dye wastewater has the characteristics of complex composition, deep color and difficult to be degraded. Most of dyes and their intermediate metabolites have mutagenicity, carcinogenicity and other toxicity, which seriously affect the ecological environment and human health [7–9]. Azo dyes account for about 70% of the total amount of dyes actually discharged into the water [10]. The discharge of these dyes not only causes pollution of natural water bodies, the death of aquatic animals and plants, the imbalance of ecosystems, but also directly harms the human body [11–13]. Congo red (CR) is a typical benzidine azo anion dye and is one of the representative pollutants in printing and dyeing wastewater. Therefore, it is necessary to deal with CR.

*Corresponding author.

Chitosan (CS) is a product of chitin deacetylation. Its amino group can be protonated into a high charge density positive ion polyelectrolyte in an acidic solution with a pH lower than 6.5, and has the property of adsorbing negatively charged colloidal particles in water. The chitosan molecular chain contains a large number of reactive hydroxyl groups and amino groups, which can undergo various chemical reactions to form various derivatives. Therefore, chitosan has good chelation, adsorption, cross-linking, bridging properties, good film formation, permeability, hygroscopicity, and can be used as an adsorbent and flocculant in water treatment [14].

Multi-walled carbon nanotubes (MWCNTs) are a one-dimensional nanomaterial with a unique hollow structure. The surface of the original multi-walled carbon nanotubes has a strong van der Waals force [15,16]. In practical applications, it needs to be modified to break the van der Waals force [17,18]. In recent years, modified multi-walled carbon nanotubes (MWCNTs) have been widely used in the field of water treatment [19,20]. The most used materials are synthetic and natural polymers in the modification of MWCNTs [21,22]. These studies show that modified multi-walled carbon nanotubes have a strong binding capacity and a large adsorption capacity, and are an ideal adsorbent material. Congo red (CR, anionic dye) is a typical benzidine anionic disazo dye with high solubility in aqueous solution. The metabolite of the dye, benzidine, is a known human carcinogen.

Based on the above analysis, the aim of the present study was to prepare CS-MWCNTs nanocomposite for removal of CR from solution. The composite material not only overcomes the disadvantage that MWCNTs and CS which are difficult to separate in solution, but also has the advantages of having a large specific surface area of MWCNTs and a large number of adsorption sites of CS. The comparison of the adsorption capacity of CR with other adsorbents is shown in Table 1 [23–28]. It shows that CS-MWCNTs has a higher adsorption capacity for CR. In addition, CS-MWCNTs were simple to prepare, environmentally friendly, and recyclable. The effect of pH and salt concentration on the adsorption quantity was determined and the mechanism of adsorption was presented in the study.

2. Materials and methods

2.1. Materials

Multi-walled carbon nanotubes (MWCNTs, Macklin, Shanghai, China. ID: 5–10 nm, OD: 10–30 nm, length: 10–30 um, purity: >90%), chitosan (CS, deacetylation degree greater than or equal to 90%, SCRC, Shanghai, China), acetic acid (Bodi Chemical Reagent, Tianjin, China), ammonium hydroxide (w%: 25%–28%, Sinopharm Chemical Reagent,, Yantai, China), congo red (CR, Aladdin, Shanghai, China). The chemicals used in the experiments were of analytical grade. Distilled water is used.

Table 1
Comparison of monolayer adsorption capacity of CR onto various adsorbents

Adsorbent	q_e (mg·g^{-1})	Reference
$Fe(OH)_3$ microspheres	308	[23]
Raw-chitosan	114	[24]
Bentonite	19	[25]
Pepper stalk waste	6.5	[26]
Magnetic Diatomite	226	[27]
Organic sepiolite	246	[28]
CS-MWCNTs	623	This study

2.2. Preparation of CS-MWCNTs

0.1 g of chitosan was dissolved in 100 ml of 1% acetic acid solution and 0.1 g of MWCNTs was added, then was ultrasonically dispersed for 2 h. The 5 ml ammonia (w%: 25%) solution was added dropwise to the black mixtures, and MWCNTs and CS were coagulated and precipitated completely, and the pH of the solution was about 10 [29]. The black precipitate was filtered and washed with ultrapure water until the filtrate was neutral. Finally, the CS-MWCNTs composite was dried in a blast oven at 60°C for 8 h, then cooled and ground for later use.

2.3. Characterization of MWCNTs and CS-MWCNTs

Several analytical techniques were used to characterize the synthesized materials. The microstructure and morphology of MWCNTs and CS-MWCNTs were imaged by transmission electron microscope (TEM, TECNAIG2F20-S-TWIN, America). The MWCNTs and CS-MWCNTs were dispersed by ultrasonication in ethanol, and the dispersed solution was dropped onto a copper grid for measurement.

The characteristic functional groups were determined by Fourier transform infrared spectroscopy (FT-IR Spectrometer, Nicolet iS50, American). The spectral range is 500–4000 cm^{-1}, resolution is 0.09 cm^{-1}, and sample concentration is 1% (w%).

Raman spectroscopy (Raman, LabRAM HR Evolution, France) was used to determine the structure of MWCNTs and CS-MWCNTs. The wavelength of laser is 532 nm, spectral range is 500–2500 cm^{-1}, resolution is 0.03 cm^{-1}.

The binding energy of CS-MWCNTs adsorbed CR before and after was analyzed by X-ray photoelectron spectroscopy (XPS, ESCALAB 250Xi, England). The type of the X-ray source is Al (hv = 1486.6 eV), and it is monochromatic. The survey scan range is 0–1000 eV, dwell time is 340 s, pass energy is 20 eV, step size is 0.05 eV and number of sweeps is 5.

Analysis of material surface charge changes by pHpzc. The pH of 10 ml of 0.01 mol·L^{-1} NaCl solution was adjusted to between 2 and 11, and 0.01 g of CS-MWCNTs was added to the NaCl solution for an equilibrium time of 720 min. Then measure the final pH of the solution as pH_{final}. The pHpzc is the point where $pH_{intial} - pH_{final} = 0$.

2.4. Adsorption experiments

The CR adsorption onto CS-MWCNTs was performed in batch mode. 6.0 mg of CS-MWCNTs was added to a 50 ml conical flask, and 10 ml of a 400 mg·L^{-1} CR solution was added. The conical flask was placed in a 120 rpm thermostat shaker (Guohua Enterprise SHZ-82, China). After adsorption, CS-MWCNTs were separated by centrifugation at 3000 rpm. The absorbance of CR in the supernatant

was measured twice, and the concentration was calculated using the CR standard curve of the maximum wavelength (499 nm), and the average of the two calculations was taken as the CR concentration (752, SDPTOP, China). The error of determination is less than 5%.

The influencing factors include: (1) the effect of pH: the pH value of CR solution was adjusted to a range of 3–11, at 303 K; (2) the effect of salt concentration: inorganic salts of different kinds and different concentrations are added to the CR solution, at 303 K, pH = 4; (3) effect of contact time and concentration: the concentration of CR solution was adjusted to 300 mg·L^{-1}, 400 mg·L^{-1}and 500 mg·L^{-1}, the range of adsorption time was from 5 min to 480 min, at 293 K, 303 K, 313 K, pH = 4; (4) effect of dye concentration and temperature: the initial concentration of the CR solution was adjusted to a range of 200–750 mg·L^{-1}, at 293 K, 303 K, 313 K, pH = 4. All tests were double and average was selected.

The adsorption quantity of CR loaded onto unit mass of CS-MWCNTs was calculated using equation:

$$q_e = \frac{V(C_0 - C_e)}{m} \quad (1)$$

where V is the CR solution volume (L), C_0 is the initial CR concentration (mg·L^{-1}), C_e is the CR concentration at any time t or equilibrium (mg·L^{-1}), and m is the mass of CS-MWCNTs (g).

2.5. Desorption study

The CR-loaded CS-MWCNTs was prepared by CS-MWCNTs adsorption of 400 mg·L^{-1} of CR (pH = 4.0, T = 303 K, solid-liquid ratio is 0.6 g·L^{-1}), and then the CR-loaded CS-MWCNTs were washed with distilled water to remove the unadsorbed dye and were dried at 60°C in heating oven. The CR loaded-CS-MWCNTs was desorbed by different methods (75% ethanol, NaOH solution and microwave irradiation), and the CS-MWCNTs were washed and dried after desorption, and the adsorption experiments were repeated under the same conditions. The best desorption method was used to repeated desorption and regeneration experiments.

3. Results and discussion

3.1. Characterization of MWCNTs and CS-MWCNTs

3.1.1. TEM analysis

The TEM images of MWCNTs and CS-MWCNTs are shown in Fig. 1. It is observed from Fig. 1a that MWCNTs has good dispersibility on the surface, no impurities. Fig. 1b shows that the surface of carbon nanotubes in CS-MWCNTs was covered by chitosan, and the dispersibility of MWCNTs was reduced.

3.1.2. FTIR analysis

FTIR is one of the most important characterization techniques for elucidating chemical structural changes. FTIR of CS, MWCNTs and CS-MWCNTs are illustrated in Fig. 2. It was observed from Fig. 2 that a broad peak of CS, MWCNTs and CS-MWCNTs appeared at 3437 cm^{-1} due to stretching vibration of –OH or –NH. CS and CS-MWCNTs possessed main peaks at 2920 cm^{-1} due to the bending vibrations of –CH_2. The absorption peak at 1644 cm^{-1} was a characteristic absorption peak of C–N vibration [30]. The absorption at 1000 to 1200 cm^{-1} comes from the vibration of the C–O. The main difference in the infrared spectrum of CS-MWCNTs and MWCNTs was that the peak at 3437 cm^{-1} from –OH or –NH stretching vibration was enhanced (Fig. 2). This indicated that a large amount of amino or hydroxyl groups were introduced on the surface of MWCNTs.

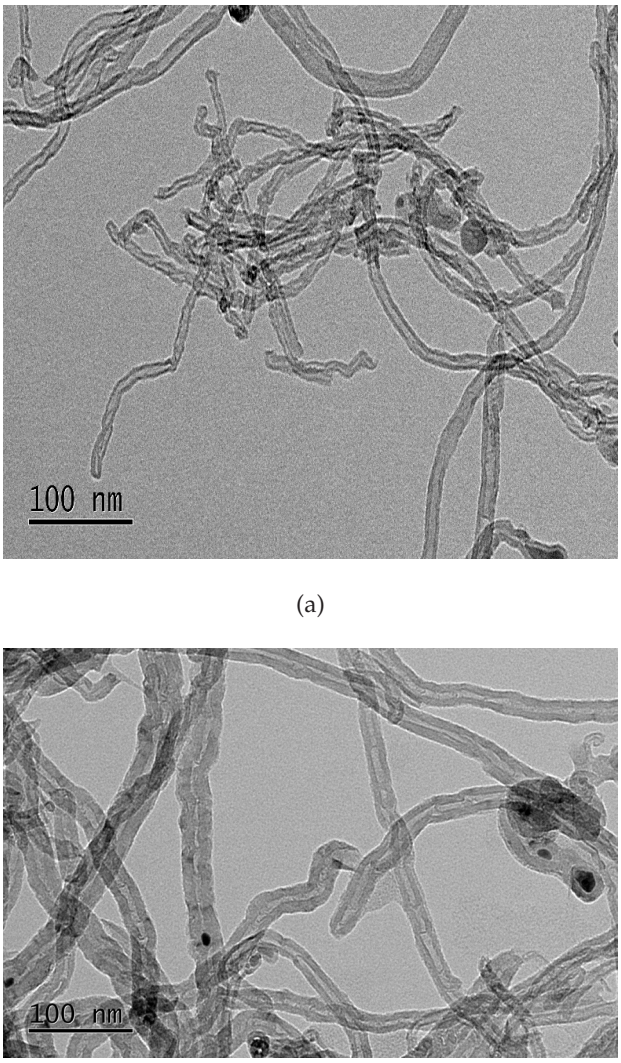

(a)

(b)

Fig. 1. TEM images of MWCNTs (a) and CS-MWCNTs (b).

3.1.3. Raman analysis

Raman of adsorbent can offer some useful information. Fig. 3 shows the Raman spectra of MWCNTs and CS-MWCNTs. There are two peaks at 1353 cm^{-1} and 1593 cm^{-1} according to Fig. 3, which correspond to the vibration caused by the disordered structure and the defects of the

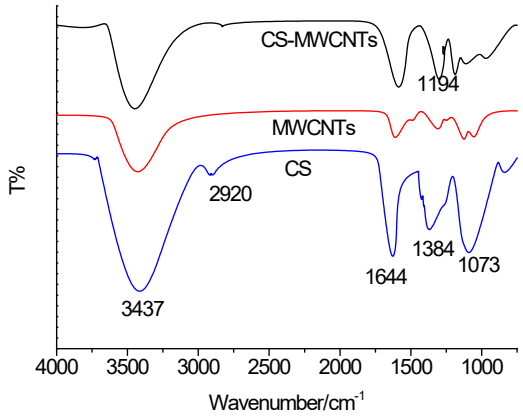

Fig. 2. FTIR spectra of CS, MWCNTs and CS-MWCNTs.

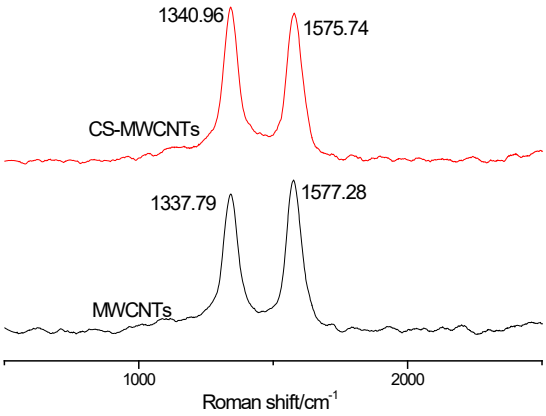

Fig. 3. Raman spectra of MWCNTs and CS-MWCNTs.

graphite (point D), and the vibration between the carbon and carbon in the plane of the aromatic configuration layer of the graphite (point G). The area ratio of the two absorption peaks (ID/IG) represents the order degree of the carbon nanotubes' surface (disturbance degree) [31]. The ID/IG values of MWCNTs and CS-MWCNTs are 1.028 and 1.027, respectively. Compared with MWCNTs, the IG/ID value of CS-MWCNTs does not change much, indicating that the structure of carbon nanotubes is basically unchanged during the modification process. The carbon atoms on the carbon nanotubes do not react, and the reaction only occurs on the functional groups.

The process of CS modified MWCNTs is through non-covalent functionalization to modify the MWCNTs surface by wrapping the MWCNTs with CS, or by adsorption of CS on the MWCNTs surface via π–π interactions, electrostatic interaction or hydrophobic effects [23,32].

3.1.4. XPS analysis

The surface chemistry of CS-MWCNTs and CR-loaded CS-MWCNTs was investigated using XPS (Fig. 4). It was seen from the general spectrum that CS-MWCNTs mainly contained C, O, N elements, of which N element was

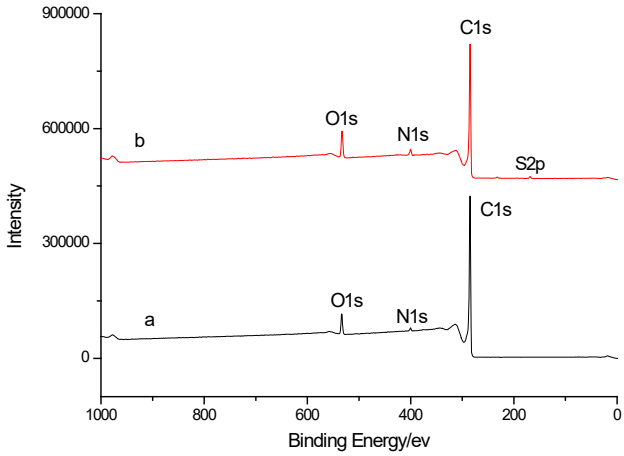

Fig. 4. The survey XPS spectra of CS-MWCNTs (a) and CS-MWCNTs /CR (b).

mainly from CS introduction. The elemental contents were 93.22% C, 5.1% O, and 1.68% N, respectively. XPS analysis provided further evidence for the successful preparation of CS-MWCNTs. Fig. 4b is a full spectrum of CR-loaded CS-MWCNTs. After CR adsorption on CS-MWCNTs, the weak peak of S2p appeared at 168.5 eV, indicating that CR was adsorbed on the surface of CS-MWCNTs.

3.1.5. Zero point of charge

The zero point of charge of materials indicated the functional groups on their surface and the results are shown in Fig. 5. It was seen from Fig. 5 that the pH_{pzc} values were 6.6 for CS-MWCNTs. When the pH of the CR solution is higher than 6.6, the surface of the material is negatively charged, and below 6.6, the surface of the material is positively charged. And when the solution pH is higher than 4, the positive charge on the surface of the material is gradually reduced.

3.2. Batch adsorption studies

3.2.1. The effect of pH on adsorption

The pH of the solution often affects the charge on the surface of the adsorbent as well as the chemical structure and stability of adsorbate. Fig. 6 shows the effect of solution pH on CR adsorption. It was seen that it was favored of CR adsorption at solution pH 4.0. When solution pH was over or less than 4.0, the adsorption quantity decreased, so working solution pH was adjusted to 4 in the following experiments. When solution pH is less 4.0, some chitosan is dissolved and the material is destroyed, so values of q_e became less. CR is an anionic dye with negative charge and there was positive charge on the surface of adsorbent. The adsorption force is mainly electrostatic attraction. With solution pH increased, the electrostatic force was weakened and the adsorption capacity of CS-MWCNTs decreased. Similar result was obtained about CR adsorption onto raw chitosan [24] and chitosan coated magnetic iron oxide [33]. But the trend about effect of solution pH was different about light green adsorption onto PEI-modified MWCNTs [20].

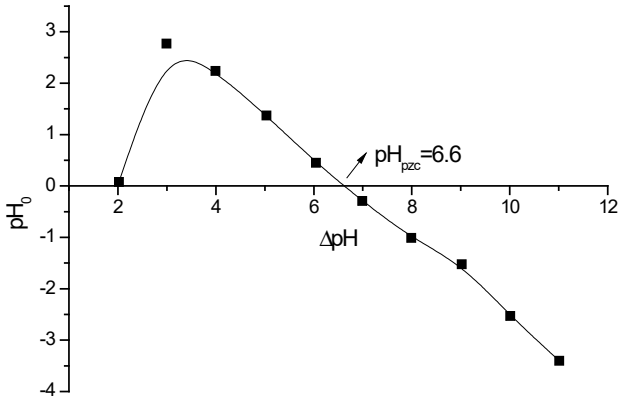

Fig. 5. Plots of ΔpH against initial pH for the determination of pHpzc of CS-MWCNTs.

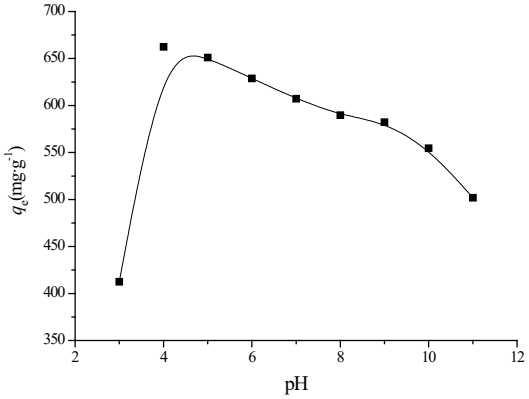

Fig. 6. Effect of solution pH on CR adsorption (T = 303 K, C_0 = 400 mg·L^{-1}, CS-MWCNTs dosage = 0.6 g·L^{-1}, contact time 480 min).

Under the same conditions (adsorption dose 0.6 g·L^{-1}, C_0 = 400 mg·L^{-1}, pH = 4.0, t = 480 min, T = 303 K), MWCNTs and CS-MWCNTs have q_e value of 286.8 mg·g^{-1} and 623.3 mg·g^{-1}, respectively. But the adsorption quantity of CS toward CR was 114 mg·g^{-1} from isotherm curve [24]. This confirmed that the MWCNTs adsorption capacity after CS modification was significantly enhanced. So the modification is valuable.

But even at solution pH 2.0 or higher solution pH, values of q_e were still over 400 mg·g^{-1} (Fig. 6) and was higher than that of MWCNTs. This showed that there were other action between CR and CS-MWCNTs, such as hydrogen bonding and van der Waals force [33].

3.2.2. The effect of salt concentration on adsorption

In the actual process of wastewater treatment, the wastewater usually contains other coexisting inorganic salt ions, which may affect the adsorption amount. Therefore, it is necessary to discuss the influence of salinity on adsorption quantity and the results of salt effect are presented in Fig. 7. It was seen from Fig. 7 that when the concentration of NaCl, Na_2SO_4 and $CaCl_2$ increased from 0 to 0.10 mol·L^{-1}, the adsorption increased from 623 mg·g^{-1} to 653 mg·g^{-1}, 648 mg·g^{-1} and 663 mg·g^{-1} respectively. The effect of $NaHCO_3$ decreases first and then increases slowly, because the presence of $NaHCO_3$ increases the value of the pH of the solution. This indicated that the presence of inorganic salt ions is beneficial to the adsorption process. During the experiment, it was found that some CR molecules settled on the surface of the CS-MWCNTs during the adsorption process. The reason may be that in the process of CR adsorption onto CS-MWCNTs, the addition of salt reduces the thickness of the electric double layer, making the diffusion of the dye to the adsorbent easier. This facilitates adsorption of CR by electrostatic attraction, thereby increasing the amount of the dye adsorption.

Similar results were obtained about CR adsorption on onto chitosan coated magnetic iron oxide [33] and ethylenediamine and the modified wheat straw [34]. But the opposite trend was observed about methyl ooange adsorption onto chitosan coated sand [32].

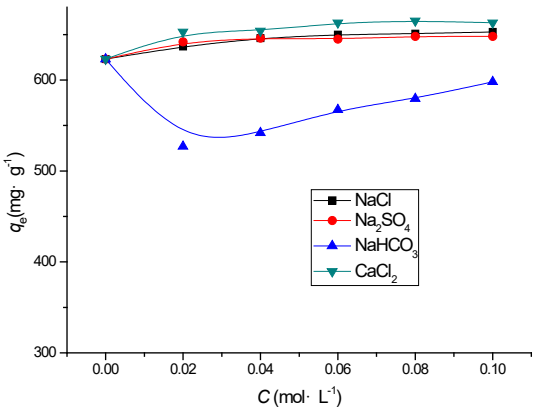

Fig. 7. Effect of NaCl and Na_2SO_4 concentration on CR adsorption (T = 303 K, C_0 = 400 mg·L^{-1}, pH = 4.0, CS-MWCNTs dosage = 0.6 g·L^{-1}, t = 480 min).

3.2.3. The effect of equilibrium concentration and temperature on adsorption

The effect of equilibrium concentrations of CR and adsorption temperatures are recorded in Fig. 8. It was shown that the value of q_e increased with the increase in CR concentrations. As the equilibrium concentration of CR increased, the surface adsorption site of CS-MWCNTs was decreased relatively. It could be seen that the value of q_e increased with the increase of temperatures. The results indicated that the adsorption process was endothermic and the increase in temperature was favorable of CR adsorption. This may be due to that the increase in temperature promotes the acceleration of molecular motion, resulting in easier access of CR molecules to more adsorption sites [33].

The surface properties of the adsorbent and the interaction between the adsorbent and the adsorbate can be known depending on the type of adsorption isotherm. The experimental adsorption isotherms can be described by the adsorption isotherm equation, and the adsorption mechanism can be better explained theoretically by obtaining different model parameters. Three common isothermal

adsorption models were used, Langmuir, Freundlich and Koble-Corrigan models.

The Langmuir adsorption isotherm describes monolayer adsorption, the Langmuir isotherm can be expressed as [35]:

$$q_e = \frac{q_m K_L c_e}{1 + K_L c_e} \quad (2)$$

where q_e (mg·g^{-1}) represents the amount of adsorbed per unit mass of adsorbent, q_m (mg·g^{-1}) denotes the saturated adsorption amount, c_e (mg·L^{-1}) is the equilibrium concentration and K_L (L·mg^{-1}) is a constant that is related to the binding energy.

The Freundlich isotherm indicates that the adsorption process is heterogeneous multi-layer adsorption. The Freundlich isotherm is usually expressed as [36,37]:

$$q_e = K_F c_e^{1/n} \quad (3)$$

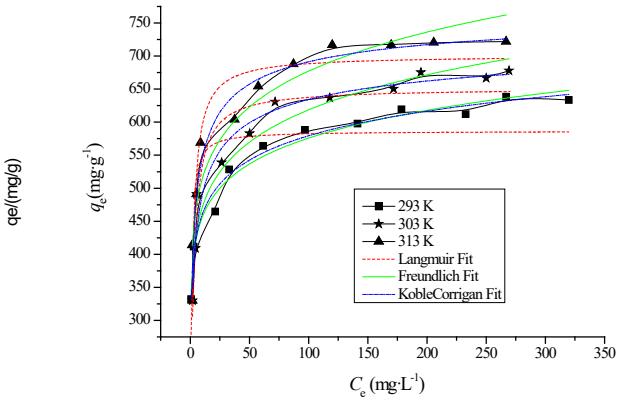

Fig. 8. Adsorption isotherms and fitted curves of CR adsorption onto CS-MWCNTs.

where K_F (L·g^{-1}) and n are the Freundlich constants characteristic of the system, which are related to the adsorption capacity and adsorption intensity of the sorbent, respectively.

The three-parameter Koble-Corrigan equation which is a combination of the Langmuir and Freundlich isotherm type models. It is given by equation [38]:

$$q_e = \frac{AC_e^n}{1 + BC_e^n} \quad (4)$$

where A (L·mg^{-1}), B (L·mg^{-1}) and n are the Koble-Corrigan parameters.

The experimental data of CR adsorption onto CS-MWCNTs at different temperatures were nonlinearly fitted to the above equations, combined with error analysis. The fitted results are shown in Table 2 and the fitted curves are also presented in Fig. 8.

For Langmuir model, the maximum adsorption amount of CS-MWCNTs towards CR was 580 mg·g^{-1}, 643 mg·g^{-1}, 700 mg·g^{-1}, respectively, which is quite different from the experimental result $q_{e(exp)}$. Furthermore, there were lower values of R^2 and higher values of *SSE*. The fitted curves were also far from experimental curves. So it was referred that this model be not suitable to describe CR adsorption onto CS-MWCNTs. Therefore, the Langmuir model can not be applied to predict the equilibrium process and the adsorption was not monolayer.

For Freundlich model, values of K_F (related to adsorption capacity) became larger with the increase of temperature, indicating that the adsorption was an endothermic reaction. There were higher values of R^2 and smaller values of *SSE*, while the fitted curves were closer to experimental curves, this model could describe the equilibrium process. So CR adsorption onto CS-MWCNTs was considered as a heterogeneous multi-molecular layer adsorption process. In literature, it was reported that the adsorption isotherms

Table 2
Parameters of adsorption isotherm models for CR adsorption onto CS-MWCNTs at different temperatures

Langmuir					
T (K)	$q_{m(theo)}$(mg·g^{-1})	$q_{e(exp)}$/(mg·g^{-1})	K_L (L·g^{-1})	R^2	$SSE \times 10^3$
293	580±20	633	1.50±0.52	0.703	24.5
303	643±14	675	0.473±0.073	0.919	8.82
313	700±20	721	0.557±0.10	0.894	16.8
Freundlich					
T (K)	K_F (L·g^{-1})	$q_{e(exp)}$/(mg·g^{-1})	$1/n$	R^2	$SSE \times 10^3$
293	358±9.7	633	0.104±0.0060	0.977	1.88
303	359±21	675	0.119±0.014	0.912	9.55
313	381±23	721	0.129±0.014	0.915	13.4
Koble-Corrigan					
T (K)	A (L·mg^{-1})	B (L·mg^{-1})	n	R^2	$SSE \times 10^3$
293	455±114	0.288±0.034	0.152±0.065	0.976	1.74
303	474±72	0.657±0.085	0.511±0.16	0.948	4.89
313	546±70	0.661±0.011	0.454±0.17	0.935	8.96

Note: $SSE = \sum (q - q_c)^2$, q and q_c are the experimental value and calculated value according the model, respectively.

of various anilinic compounds, aromatic compounds and dyes onto activated carbon cloth followed the Freundlich isotherm model [39,40]. According to Table 2, values of $1/n$ were between 0.1 and 0.5, indicating that CS-MWCNTs had good adsorption performance for CR.

For Koble-Corrigan model, the value of n was far from 1, this indicated that the isotherm was closer to the Freundlich modle. The value of R^2 is greater than 0.9 and the value of *SSE* is small. So Koble-Corrigan model can also be used to describe the adsorption equilibrium behavior according to the results obtained from Fig. 8 and Table 2.

3.2.4. The effect of contact time on adsorption

The effects of contact times on the adsorption of CR by CS-MWCNTs were studied at 293, 303 and 313 K, respectively. The experimental results are shown in Fig. 9.

It was found from Fig. 9 that values of q_t increased quickly with the beginning of adsorption at three temperatures. After 100 min, the values of q_t gradually increased. Over 200 min, the adsorption rate became slow and finally reached equilibrium. Values of q_t became larger at same time with the increase of temperature and there was advantage of CR adsorption at higher temperatures.

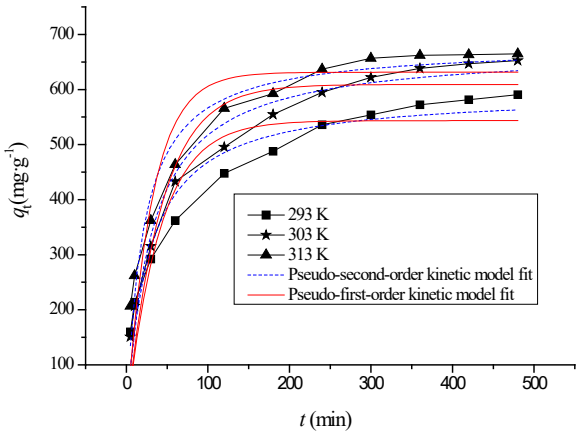

Fig. 9. Effect of contact time and concentration on adsorption quantity and kinetic fitted curves (C_0 = 400 mg·L^{-1}).

The results also showed that kinetics of CR adsorption consisted of two phases: an initial rapid phase where adsorption was fast and contributed significant to equilibrium uptake and a slower second phase whose contribution to CR adsorption was relatively small. The first phase was the instantaneous adsorption stage or external surface adsorption. The second phase was the gradual adsorption stage and finally CR uptake reached equilibrium. At same CR concentration, the time to equilibrium became shorter.

Two kinetic models of pseudo-first-order kinetic model and pseudo-second-order kinetic model are used to fit the kinetic data.

The pseudo-first order kinetic model [41]:

$$q_t = q_e(1 - e^{-k_1 t}) \tag{5}$$

The pseudo-second order equation can be expressed as [42]:

$$q_t = \frac{k_2 q_e^2 t}{1 + k_2 q_e t} \tag{6}$$

where q_t (mg·g^{-1}) is the adsorption capacity at time (t) and q_e (mg·g^{-1}) is the adsorption capacity at equilibrium; k_1 (min^{-1}) and k_2 (g·mg^{-1}·min^{-1}) are the rate constant.

The kinetic data are fitted by nonlinear regression analysis and the fit curves are also illustrated in Fig. 9. The parameters of kinetic models are listed in Table 3. It was seen from Fig. 9 and Table 3 that there were higher values of R^2 (0.95 and lower values of *SSE*) while the fitted curves were closer to experimental curves about pseudo-second-order kinetic model. This showed that the pseudo-second-order kinetic model was more suitable to predict the kinetic process of CR adsorption onto CS-MWCNTs than pseudo-first-order kinetic model. And the fitting result of the pseudo-first-order kinetic model was relatively poor, which indicated that the model was not suitable for describing the kinetic process.

3.3. Thermodynamic parameters of adsorption

In order to estimate the effect of temperature on the adsorption of CR onto CS-MWCNTs, the free energy change ($\Delta G°$), enthalpy change ($\Delta H°$), and entropy change ($\Delta S°$)

Table 3
Parameters of kinetic models for CR adsorption onto CS-MWCNTs (C_0 = 400 mg·L^{-1})

Pseudo-first-order kinetic model					
T (K)	$q_{e(exp)}$ (mg·g^{-1})	$q_{e(theo)}$ (mg·g^{-1})	$k_1\times10^{-2}$ (min^{-1})	R^2	$SSE\times10^3$
293	581	543±25	2.46±0.56	0.862	3.72
303	623	610±23	2.36±0.42	0.920	2.95
313	656	631±24	3.20±0.64	0.881	3.88
Pseudo–second–order kinetic model					
T (K)	$q_{e(exp)}$ (mg·g^{-1})	$q_{e(theo)}$ (mg·g^{-1})	$k_2\times10^{-5}$ (mg·g^{-1}·min^{-1})	R^2	$SSE\times10^3$
293	581	595±23	6.0±1.0	0.942	1.56
303	623	674±20	5.0±0.8	0.974	0.954
313	656	681±19	7.0±1.0	0.958	1.36

were calculated. The apparent equilibrium constant (K_c') of the adsorption is defined as [43]:

$$K_c' = C_{ad,e}/C_e \quad (7)$$

where $c_{ad,e}$ (mg·L^{-1}) is the concentration of CR on the adsorbent at equilibrium. The value of K_c' can be obtained with the lowest experimental CR concentration. The value of K_c' was used in the following equation to determine the Gibbs free energy change of adsorption ($\Delta G°$).

$$\Delta G° = -RT \ln K_c' \quad (8)$$

The value of $\Delta H°$ (kJ·mol^{-1}) and $\Delta S°$ (J·mol^{-1}·K^{-1}) can be obtained from the intercept and slope of van't Hoff plot of $\Delta G°$ and T:

$$\Delta G° = \Delta H° - T\Delta S° \quad (9)$$

where $\Delta G°$ (kJ·mol^{-1}) is standard Gibbs free energy change, R is universal gas constant, 8.314 J·mol^{-1}·K^{-1} and T (K) is absolute temperature.

The thermodynamic parameters were calculated and are listed in Table 4. At the experimental temperature, negative value of $\Delta G°$ indicated that the adsorption process is spontaneous. Positive value of $\Delta H°$ indicated the endothermic process, and also indicated that high temperature favored adsorption. The positive value of $\Delta S°$ indicated that the process was the increase of entropy, which indicated that the randomness of the solid solution interface increased during process of CR adsorption on CS-MWCNTs, mainly reflecting the additional translational entropy obtained by the solvent molecule.

3.4. Desorption and regeneration experiments

Reuse of spent adsorbent and recovery of adsorbate will make the treatment process economical and it is necessary to recover the adsorbent after adsorption [44,45]. The regeneration efficiency was calculated by dividing the adsorption amount of the adsorbent after the treatment by the first adsorption amount. The adsorption amount of the first adsorption saturation is q_0, the adsorption amount of the adsorbent regeneration is q_n (n is the number of regenerations), and the mass of the adsorbate remaining on the adsorbent after analysis is m_0, and the mass of the adsorbed mass is m_d. The resolution $d(\%)$ and the regeneration rate $r(\%)$ of the adsorbent can be calculated by the Eqs. (10) and (11):

$$d = \frac{m_d}{m_0} \times 100\% \quad (10)$$

Table 4
Thermodynamic parameters of CR adsorption onto CS-MWCNTs

ΔH° (kJ·mol^{-1})	ΔS° (J·mol^{-1}·K^{-1})	ΔG° (kJ·mol^{-1})		
		293 K	303 K	313 K
6.10	68.6	–14.0	–14.7	–15.4

$$r = \frac{q_n}{q_0} \times 100\% \quad (11)$$

The experimental results using various methods are shown in Fig. 10. It was seen from Fig. 10 that the regeneration efficiency of CR-loade CS-MWCNTs with 0.01 mol·L^{-1} NaOH was the best, and the regeneration rate can reach 80%. This may be due to the fact that in the alkaline solution, $-NH_3^+$ is deprotonated, the electrostatic attraction between the adsorbent and CR became weak, and the adsorbed dye is dissolved in the solution after being desorbed from the active center, and adsorbed again due to the active point of the adsorbent.

The regeneration of three cycles was also performed using 0.01 mol·L^{-1} NaOH as desorbing agent. The results are presented in Fig. 11. It was shown that the desorption efficiency was lower 50% and decreased with the increase of cycle. The regenerated efficiency became lower but it was still to 71 % after 3 cycles. In general, there is some potential use as practical and renewable adsorbents.

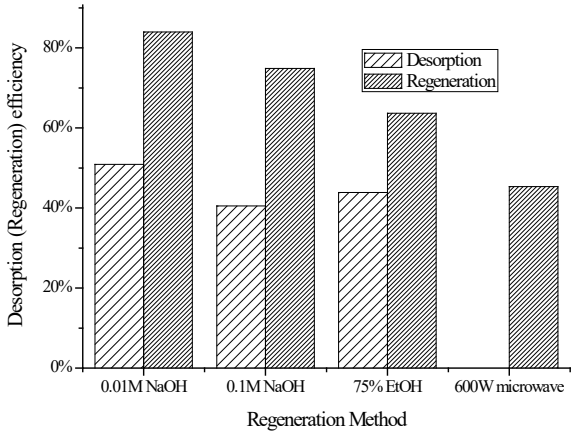

Fig. 10. Comparison of several regeneration methods after adsorption of Congo red.

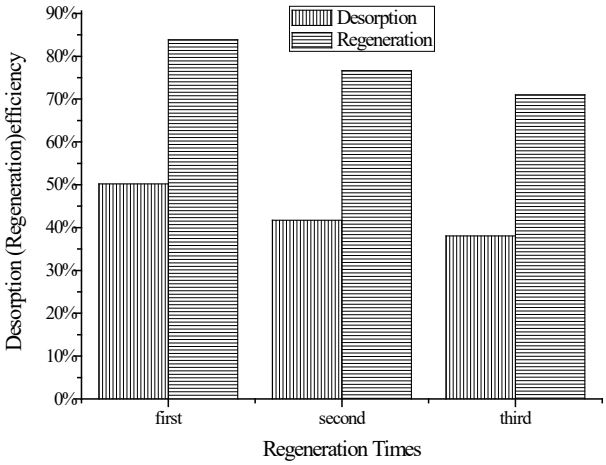

Fig. 11. Comparison of the number of regenerations after Congo red adsorption.

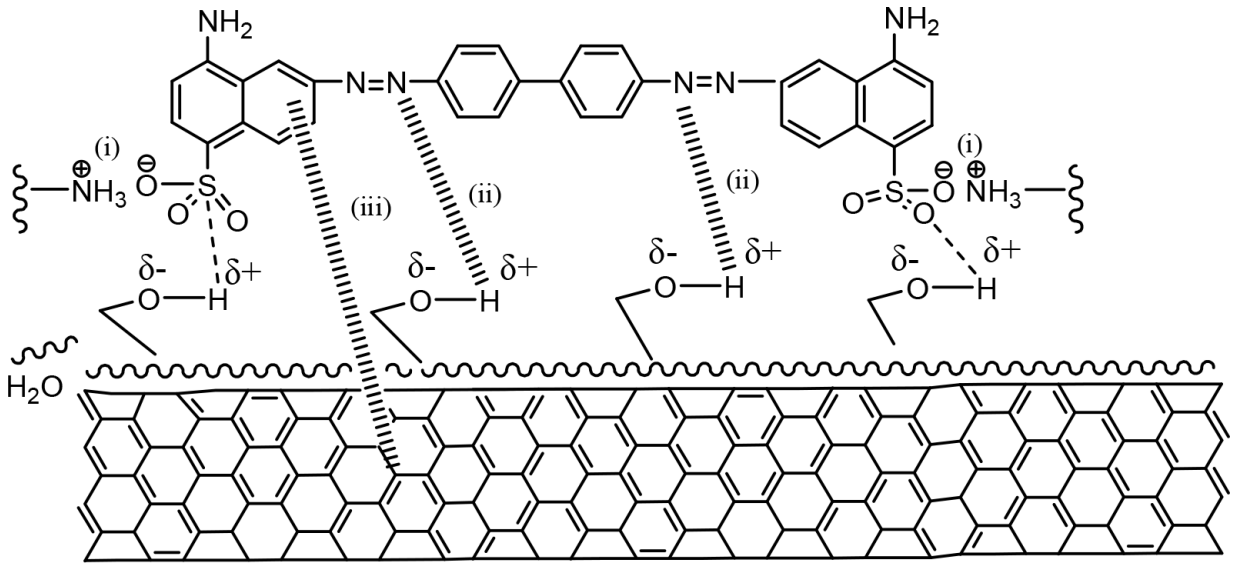

Fig. 12 (i) Inter-ion interaction, (ii) Formation of hydrogen bonds between hydroxyl groups on chitosan and N on CR molecule, (iii) Formation of hydrogen bonds between hydroxyl groups on chitosan and benzene rings in CR molecules, (iv) π-π electron stacking between benzene rings.

Low desorption efficiency of CR with pH change indicates that physical forces such as hydrogen bonding and van der Waals force may play main role in the removal of CR by CS-MWCNTs because the change in pH only affects the surface charge of the adsorbent [44].

3.5. Mechanism of CR adsorption

CS-MWCNTs was increased the adsorption abilities by introduction of amino and hydroxyl functional groups, and this preserves the integrity of the MWCNTs and reserves their exceptional properties. In addition, CS-MWCNTs are easier to separate than MWCNTs.

There are $–SO_3^-$ and $–NH_2$ groups of CR, when the pH is lowered, the surface of the adsorbent and the $–NH_2$ on the CR molecule are protonated to $–NH_3^+$ and there is electrostatic attraction between CR and CS-MWCNTs. The amount of $–NH_3^+$ on the surface of the CS-MWCNTs decreases at solution pH over 4 and this results in lower values of adsorption quantity. N, S, O from CR ion can also form hydrogen bonds with chitosan on the surface of the adsorbent, which is adsorbed by chelation [33]. There is a π-π electron stacking, between the benzene ring of CR and the benzene ring of carbon nanotubes. The mechanism of CR adsorption on CS-MWCNTs is shown in Fig. 12. Some CR molecules flocculate on the surface of the adsorbent at a suitable pH, indicating that a certain flocculation occurs at the same time of adsorption. Therefore, the adsorption mechanism contains a certain adsorption bridging effect. In addition, there are certain exposed carbon nanotubes on the surface of the adsorbent, which may also cause physical adsorption.

4. Conclusion

CS-MWCNTs have been successfully prepared and used to adsorb CR from solution in batch mode. The pH solution pH at 4.0 was favor of adsorption and there was higher adsorption capacity (623 $mg \cdot g^{-1}$ at 303K). The presence of salt promotes adsorption. The Freundlich and Koble-Corrigan models fit the equilibrium data well, and the pseudo second-order kinetic model can better describe the CR adsorption process, indicating that the adsorption is a heterogeneous multi-molecular layer and a chemisorption process. Adsorption is spontaneous and endothermic. Regeneration of CR-loaded CS-MWCNTs by NaOH solution is effective, and CS-MWCNTs can be reused. Therefore, it can be concluded that CS-MWCNTs is an effective and viable alternative to removing Congo red from wastewater.

References

[1] Z.H. Huang, Y.Z. Li, W.J. Chen, J.H. Shi, N. Zhang, X.J. Wang, Z. Li, L.Z. Gao, Y.X. Zhang, Modified bentonite adsorption of organic pollutants of dye wastewater, Mater. Chem. Phys., 202 (2017) 266–276.

[2] T.A. Nguyen, R.S. Juang, Treatment of waters and wastewaters containing sulfur dyes: A review, Chem. Eng. J., 219 (2013) 109–117.

[3] V. Nair, R. Vinu, Peroxide-assisted microwave activation of pyrolysis char for adsorption of dyes from wastewater, Bioresour. Technol., 216 (2016) 511–519.

[4] X. Xu, B.Y. Gao, B. Jin, Q.Y. Yue, Removal of anionic pollutants from liquids by biomass materials: A review, J. Mol. Liq., 215 (2016) 565–595.

[5] E. Ayranci, O. Duman, In-Situ UV-Visible spectroscopic study on the adsorption of some dyes onto activated carbon cloth, Sep. Sci. Technol., 44 (2009) 3735–3752.

[6] O. Duman, S. Tunç, T.G. Polat, Adsorptive removal of triarylmethane dye (Basic Red 9) from aqueous solution by sepiolite as effective andlow-cost adsorbent, Micropor. Mesopor. Mater., 210 (2015) 176–184.

[7] S. Nadeem, N.S. Akbar, Influence of radially varying MHD on the peristaltic flow in an annulus with heat and mass transfer, J. Taiwan Inst. Chem. Eng., 41 (2010) 286–294.

[8] N.M. Mahmoodi, F. Najafi, U. Sadeghi, B. Hayati, F. Najafi, Synthesis of cationic polymeric adsorbent and dye removal isotherm, kinetic and thermodynamic, J. Ind. Eng. Chem., 20 (2014) 2745–2753.
[9] M.N. Asl, N.M. Mahmodi, P. Teymouri, P. Teymouri, B. Shahmoradi, R. Rezaee, A. Maleki, Adsorption of organic dyes using copper oxide nanoparticles: isotherm and kinetic studies, Desal. Water Treat., 46 (2016) 1–10.
[10] K.V. Radha, V. Sridevi, K. Kalaivani, Electrochemical oxidation for the treatment of textile industry wastewater, Bioresour. Technol., 99 (2009) 987–990.
[11] J. Yu, X. Wang, P.L. Yue, Optimal decolorization and kinetic modeling of synthetic dyes by Pseudomonas, Strains, Water Res., 35 (2001) 3579–3586.
[12] O. Duman, S. Tunç, T.G. Polat, Determination of adsorptive properties of expanded vermiculite for the removal of C. I. Basic Red 9 from aqueous solution: Kinetic, isotherm and thermodynamic studies, Appl. Clay Sci., 109–110 (2015) 22–32.
[13] O. Duman, S. Tunç, T.G. Polat, B.K. Bozoglan, Synthesis of magnetic oxidized multiwalled carbon nanotube-κ-carrageenan-Fe_3O_4 nanocomposite adsorbent and its application in cationic Methylene Blue dye adsorption, Carbohydr. Polym., 147 (2016) 79–88.
[14] M. Vakili, M. Rafatullah, B. Salamatinia, A.Z. Abdullah, M.H. Ibrahim, K.B. Tan, Z. Gholami, P. Amouzgar, Application of chitosan and its derivatives as adsorbents for dye removal from water and wastewater: A review, Carbohyd. Polym., 113 (2014) 115–130.
[15] S. Iijim, Helical microtubules of graphitic carbon, Nature, 54 (1991) 56–58.
[16] A. CSgney, C. Laurent, E. Flahaut, R.R. Bacsa, A. Rousset, Specific surface area of carbon nanotubes and bundles of carbon nanotubes, Carbon, 39 (2001) 507–514.
[17] V.K. Gupta, R. Kumar, A. Nayak, T.A. Saleh, M.A. Barakat, Adsorptive removal of dyes from aqueous solution onto carbon nanotubes: a review, Adv. Colloid Interface Sci., 193 (2013) 24–34.
[18] O.G. Apul, T. Karanfil, Adsorption of synthetic organic contaminants by carbon nanotubes: a critical review, Water Res., 68 (2015) 34–55.
[19] Y. Huang, X. Chen, Carbon nanomaterial-based composites in wastewater purification, Nano Life, 4 (2014) 1441006 (12 pages). DOI: 10.1142/S1793984414410062
[20] Y.F. Gu, M.Y. Liu, M.M. Yang, W.L. Wang, S.S. Zhang, R.P. Han, Adsorption of light green anionic dye from solution using polyethyleneimine-modified carbon nanotubes in batch mode, Desal. Water Treat., 138 (2019) 368–378.
[21] O. Duman, S. Tunç, B.K. Bozoğlan, Removal of triphenylmethane and reactive azo dyes from aqueous solution by magnetic carbon nanotube-κ-carrageenan-Fe_3O_4 nanocomposite, J. Alloy. Comp., 687 (2016) 370–383.
[22] J.S. Burt, G.F. Ebell, Organic pollutants in mussels and sediments of the coastal waters off Perth, Western Australia, Mar. Pollut. Bull., 30 (1995) 723–732.
[23] X.L. Zhao, Y.C. Su, S.B. Li, A green method to synthesize flower-like $Fe(OH)_3$ microspheres for enhanced adsorption performance toward organic and heavy metal pollutants, J. Environ. Sci., 73 (2018) 47–57.
[24] A. Zahir, Z. Aslam, M.S. Kamal, W. Ahmad, A. Abbas, R. Awwad Shawabkeh, Development of novel cross-linked chitosan for the removal of anionic Congo red dye, J. Mol. Liq., 244 (2017) 211–218.
[25] Z.Y. Sun, Y.L. Zhang, C.Y. Ma, Thermodynamics and kinetics of Congo red adsorption onto pillared bentonite, Bull. Chin. Ceram. Soc., 37 (2018) 2930–2934.
[26] X.X. Dan, X.M. Li, Adsorption of Congo red by the pepper stalk waste , Wool Text. J., 46 (2018) 51–56.
[27] L.L. Lian, J.Y. Lu, Z. Xiu, Preparation of the functional magnetic diatomite and its application in Congo red adsorption, J. Jilin Inst. Chem. Techno., 35(07) (2018) 82–85. (in Chinese)
[28] J.Y. Li, Y.S. Ma, C.P. Wang, Adsorption kinetics and thermodynamics of Congo red from aqueous solutions onto organic sepiolite, Environ. Pollut. Contr., 35 (2013) 52–56.
[29] Y.P. Dou, H.L. Liu, J.J. Peng, A green method for preparation of CNT/CS/Ag composites and evaluation of their catalytic performance, J. Mater. Sci., 51 (2016) 5685–5694.
[30] S.Y. Pu, Y.Q. Hou, C. Yan, H. Ma, H.Y. Huang, Q.Q. Shi, S. Mandal, Z.H. Diao, W. Chu, In situ coprecipitation formed highly water-dispersible magnetic chitosan nanopowder for removal of heavy metals and its adsorption mechanism, ACS Sustain. Chem. Eng., 6 (2018) 16754–16765.
[31] L.R. Hou, L. Lian, D.K. Li, G. Pang, J.F. Li, X.G. Zhang, S.L. Xiong, C.Z. Yuan, Mesoporous N-containing carbon nanosheets towards high-performance electrochemical capacitors, Carbon, 64 (2013) 141–149.
[32] B.L. Zhao, X.N. Zhang, C.C. Dou, R.P. Han, Adsorption property of methyl orange by chitosan coated on quartz sand in batch mode, Desal. Water Treat., 55 (2015) 1598–1608.
[33] H.M. Zhu, M.M. Zhang, Y.Q. Liu, L.J. Zhang, R.P. Han, Study of congo red adsorption onto chitosan coated magnetic iron oxide in batch mode, Desal. Water Treat., 37 (2012) 46–54.
[34] Z.W. Wang, P. Han, Y.B. Jiao, D. Ma, C.C. Dou, R.P. Han, Adsorption of congo red using ethylenediamine modified wheat straw, Desal. Water Treat., 30 (2011) 195–206.
[35] Y.C. Rong, H. Li, L.H. Xiao, Q. Wang, Y.Y. Hu, S.S. Zhang, R.P. Han, Adsorption of malachite green dye from solution by magnetic activated carbon in batch mode, Desal. Water. Treat., 106 (2018) 273–284.
[36] M.Y. Han, Q. Wang, H. Li, L.Y. Fang, R.P. Han, Removal of methyl orange from aqueous solutions by polydopamine mediated surface functionalization of Fe_3O_4 in batch mode, Desal. Water Treat., 115 (2018) 271–280.
[37] R.D. Zhang, J.H. Zhang, X.N. Zhang, C.C. Dou, R.P. Han, Adsorption of Congo red from aqueous solutions using cationic surfactant modified wheat straw in batch mode: Kinetic and equilibrium study, J. Taiwan Inst. Chem. Eng., 45 (2014) 2578–2583.
[38] C. Rakae, Adsorption isotherms for pure hydrocarbons, Ind. Eng. Chem., 44 (1952) 383–387.
[39] O. Duman, E. Ayranci, Structural and ionization effects on the adsorption behaviors of some anilinic compounds from aqueous solution onto high-area carbon-cloth, J. Hazard. Mater., 120 (2005) 173–181.
[40] E. Ayranci, Adsorption characteristics of benzaldehyde, sulphanilic acid, and p-phenolsulfonate from water, acid, or base solutions onto activated carbon cloth, Sep. Sci. Technol., 41 (2006) 3673–3692.
[41] Y. Liu, Y.J. Liu, Biosorption isotherms, kinetics and thermodynamics, Sep. Purif. Technol., 61 (2008) 229–242.
[42] Y.S. Ho, G. McKay, Pseudo-second-order model for sorption process, Process Biochem., 34 (1999) 451–465.
[43] Z. Aksu, Determination of the equilibrium, kinetic and thermodynamic parameters of the batch biosorption of nickel(II) ions onto Chlorella vulgaris, Process Biochem., 38 (2002) 89–99.
[44] R.P. Han, Y. Wang, Q. Sun, L.L. Wang, J.Y. Song, X.T. He, C.C. Dou, Malachite green adsorption onto natural zeolite and reuse by microwave irradiation, J. Hazard. Mater., 175 (2010) 1056–1061.
[45] Y.B. Jiao, D.L. Han, Y.Z. Lu, Y.C. Rong, L.Y. Fang, Y.L. Liu, R.P. Han, Characterization of pine-sawdust pyrolytic char activated by phosphoric acid through microwave irradiation and adsorption property toward CDNB in batch mode, Desal. Water. Treat., 77 (2017) 247–255.